Delayed Sliding Mode Control of Chaotic Systems

Baghdadi Hamidouche, Kamel Guesmi, Najib Essounbouli

Russian Journal of Nonlinear Dynamics, 2024, vol. 20, no. 2, pp. 277–293.
Full-texts are available at http://nd.ics.org.ru
DOI: 10.20537/nd240204

MATHEMATICAL PROBLEMS OF NONLINEARITY

MSC 2010: 93D15

Delayed Sliding Mode Control of Chaotic Systems

B. Hamidouche, K. Guesmi, N. Essounbouli

This paper presents a comprehensive investigation of delayed sliding-mode control and synchronization of chaotic systems. The findings of this paper offer valuable insights into chaos control and synchronization and provide promising prospects for practical applications in various domains where the control of complex dynamical systems is a critical question. In this paper, we propose three approaches of control to regulate chaotic behavior and induce synchronization between the system's state and its delayed value, by one period, of the unstable periodic orbits (UPOs). The stabilization ability of each controller is demonstrated analytically based on Lyapunov theory. Furthermore, we provide a bridge between classical stability and structural one through the use of the synchronization error, as an argument of the controller, instead of the classical tracking error.

Through three sets of simulations, we demonstrate the effectiveness of the proposed approaches in driving the chaotic system toward stable, simple, and predictable periodic behavior. The results confirm the rapid achievement of stabilization, even with changes in the sliding surface and control activation time point showing, hence, the approaches' adaptability and reliability. Furthermore, the controlled system exhibits remarkable insensitivity to changes in initial conditions, thus showing the robustness of the proposed control strategies.

Keywords: chaotic systems, sliding mode control, synchronization, time-delayed system, unstable periodic orbits, Rössler benchmark

Received September 07, 2023
Accepted December 21, 2023

Baghdadi Hamidouche
b.hamidouche@univ-djelfa.dz
LAADI, Djelfa University
Cité Ain Chih B-P 3117, Djelfa, Algeria

Kamel Guesmi
guesmi01@univ-reims.fr
Najib Essounbouli
essounbouli01@univ-reims.fr
CReSTIC, Reims University
2 Av. Robert Schuman, 51100 Reims, France

1. Introduction

Chaos theory is a significant subdivision within the broader framework of nonlinear systems theory. Chaos refers to the unpredictable, nonrepetitive, and aperiodic behavior observed in deterministic systems. One key characteristic of chaotic systems is their high sensitivity to initial conditions, characterized by a positive Lyapunov exponent. This sensitivity leads to the so-called "butterfly effect", where small changes in initial conditions can lead to vastly different long-term trajectories [1]. Indeed, chaotic systems display an exceptional degree of sensitivity not solely to their initial conditions, but also to alterations in their system parameters. Even infinitesimal shifts in initial conditions can induce significant qualitative shifts in the system's behavior, complicating, thus, the task of mastering a such kind of systems. Given this critical and complex context, a variety of control strategies have been driven to address the encountered challenges. The literature review, in this area, shows many approaches of control such as the delayed feedback control [2], the generalized predictive control [3], the fuzzy control [4], the proportional-integral technique [5], the impulsive approach [6], the adaptive control technique [7], and the sliding mode control (SMC) [8–10].

The sliding mode control is widely recognized as one of the most powerful control techniques. It has been extensively investigated for stabilizing and controlling chaotic systems. This method offers robustness against uncertainties and disturbances, rendering it particularly suitable for addressing the inherent complexity and unpredictability of chaotic dynamics. At the core of sliding mode control (SMC) is its ability to efficiently stabilize and regulate chaotic systems. This achievement is accomplished through the formulation of a sliding surface and the implementation of a control law which ensures that the system's trajectory converges to and remains on this surface.

The selection of the sliding surface holds immense importance, as it directly shapes the behavior of the system and dictates its reaction to the control signal. A well-designed sliding surface ensures the way for efficient control and stabilization of the system, enabling successful management even in the face of complex and challenging dynamics.

In the context of classical stability analysis, the error is commonly recognized as the disparity between the current state of a system and the target equilibrium point. However, in our case, we deal instead with structural stability. Consequently, the conventional tracking error will be replaced with what we called the synchronization error. This last is defined as the difference between the present state of the system and its value, delayed by exactly one period along the trajectory of the unstable periodic orbits (UPOs). This shift in focus allows us to explore the system's robustness and adaptability in synchronizing its behavior with a desired structurally stable trajectory.

Our mission is to integrate the sliding mode control technique with the delayed synchronization approach to ensure the system's structural stability. This integration uses the delayed state of the system as the reference trajectory, thereby establishing the basis for defining the sliding surface. After successfully identifying the delayed state values of the system, we make a deliberate choice to adopt one of the period values from the unstable periodic orbits (UPOs) as the designated sliding surface. Consequently, the proposed approaches introduce three distinct sliding surfaces, each one dealing with the synchronization principle.

Additionally, in order to ascertain the UPO's value, we employ the widely recognized Poincaré section technique [11]. This method involves constructing a Poincaré section through the strategic intersection of the UPO with a carefully selected plane within the phase space. The period of the UPO is determined through the measurement of the time interval between

consecutive intersections of the UPO with the Poincaré section. To substantiate the stability of the closed-loop system, the Lyapunov theory will be used. This theoretical framework will provide the necessary justification for affirming the system's stability under the proposed control laws.

The organization of this paper is as follows: In Section 2, a brief overview of the Rössler system is provided, highlighting its significance as a benchmark for chaos control. Section 3 introduces the proposed three delayed sliding-mode control approaches and presents their key concepts. Additionally, the problem formulation is detailed, outlining the objectives of synchronization and stabilization. In Section 4, the simulation results are presented and thoroughly analyzed to validate the proposed approaches and to evaluate their performance.

2. Chaotic benchmark

For validation purposes and without loss of generality we have selected, in this paper, the Rössler system as the benchmark system. The Rössler system is a well-known chaotic system widely used in the literature to assess the efficiency of various control techniques. It was introduced by Otto E. Rössler in 1976 [12] and has since become a popular choice for validation purposes of the control and synchronization techniques in chaos theory.

The dynamics of the Rössler system can be described by the following set of ordinary differential equations:

$$\begin{cases} \dot{x}(t) = -y(t) - z(t), \\ \dot{y}(t) = x(t) + ay(t), \\ \dot{z}(t) = b + z(t)(x(t) - c), \end{cases} \tag{2.1}$$

where x, y and z are the state variables and a, b and c are the system parameters. When they are chosen as $a = 0.2$, $b = 0.2$, $c = 5.7$, the attractor of the system is illustrated in Fig. 1. The blue and red curves on the attractor, depicted in Fig. 1, correspond to the system's trajectories starting from the initial conditions [0.1, 0.1, 0.1] and [0.2, 0.2, 0.2], respectively. The time evolution of the system states is shown in Fig. 2.

From Figs. 1 and 2 it is evident that the Rössler system exhibits chaotic behavior. Consequently, the system is highly sensitive to even slight changes in the initial conditions or the system parameters. This sensitivity causes the system's behavior to undergo substantial and unpredictable variations over time. In order to confirm this remark, we use Wolf's algorithm [13] to obtain the following Lyapunov exponent:

$$\lambda_1 = 0.0706, \quad \lambda_2 = 0.000 \quad \text{and} \quad \lambda_3 = -5.4005.$$

It is obvious to say that the Rössler system with these parameters is chaotic due to the positive Lyapunov exponent λ_1. Thus, the development of a control method becomes crucial to achieve structural stability and compel it to exhibit a more straightforward and predictable behavior. With this goal in mind, we will present three approaches utilizing delayed sliding-mode control techniques to achieve synchronization between the current state of the system and its delayed state by one period. The primary objective of these approaches is to structurally stabilize the system's first unstable periodic orbit (UPO).

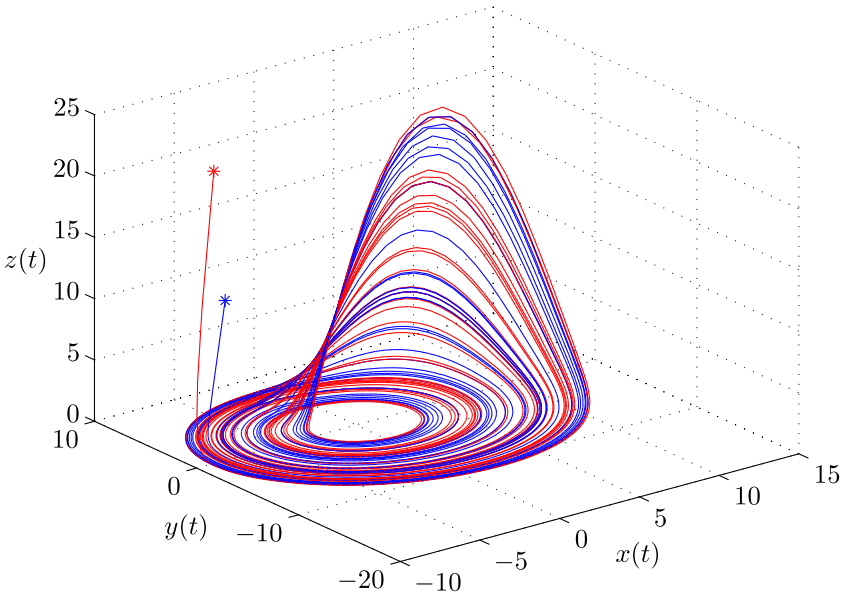

Fig. 1. Behavior of the Rössler system without control

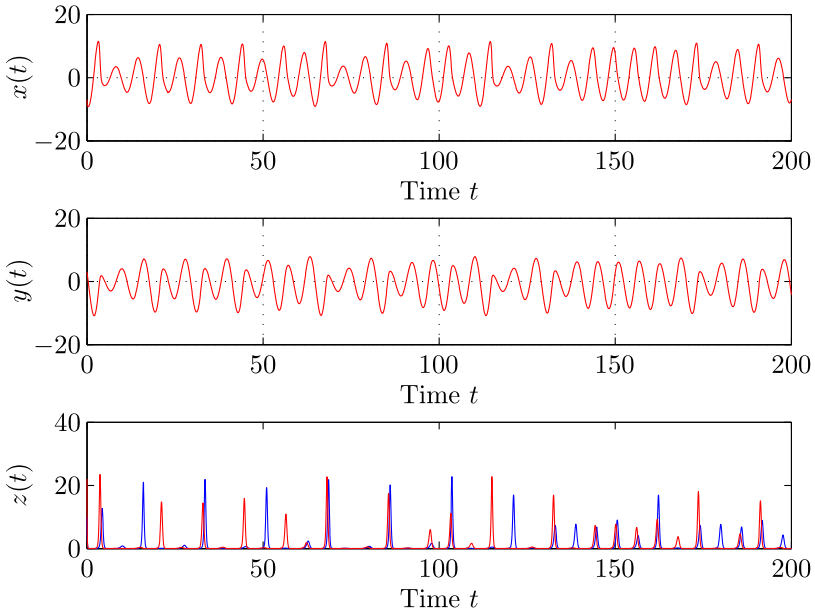

Fig. 2. Time behavior of $x(t)$, $y(t)$ and $z(t)$ states without control

3. Delayed sliding mode control

This section aims to formulate the problem of chaos control and stabilization using the delayed sliding mode control (DSMC) technique. To begin, let us consider the general form of dynamical chaotic systems given by

$$\dot{X}(t) = F(X(t),\, t) + U(t), \tag{3.1}$$

where $X \in R^n$ is the state variable, $F\colon R^n \longrightarrow R^n$ is a nonlinear function describing the system dynamics, and n is the system dimension. $U \in R^i$ denotes the control term that will be designed to stabilize the chaotic system with i the number of inputs, and $i \leqslant n$.

The fundamental concept of sliding mode control is to drive the system to track a desired or predefined trajectory by constraining its dynamics to slide along a predefined surface called the sliding surface. The latter can be formulated as a function of the state of the system and the desired trajectory.

In our study, we select the delayed state of the system as the desired trajectory. As defined in [17], the general form of the sliding surface in the state space R^n can be defined by the scalar equation $S_i(x, t) = 0$ with

$$S_i(x, t) = \left(\frac{d}{dt} + \lambda_i\right)^{n-1} e_i, \tag{3.2}$$

where e_i is the tracking error and λ is a strictly positive constant. The use of delayed states as the desired trajectory in sliding mode control allows us to achieve synchronization between the current value of the system's state and its delayed value. This synchronization is essential for stabilizing structurally the system's first unstable periodic orbit (UPO) and regulating its chaotic behavior effectively using the synchronization error instead of the conventional tracking error. To do so, let us define the synchronization error as

$$e_i = x_i(t) - x_i(t - \tau) \tag{3.3}$$

with τ the delayed time.

In the remaining subsections, we deal with the implementation and analysis of the proposed approaches. Hence, if the system's order is $n = 2$, Eq. (3.2) becomes:

$$S_i(t) = \dot{e}_i + \lambda_i e_i \tag{3.4}$$

with the control objective to obtain [15, 18, 19]:

$$\lim_{t\to\infty} S_i(t) = 0 \quad \text{and} \quad \lim_{t\to\infty} \dot{S}_i(t) = 0.$$

This means that, once the system is in the sliding phase, it remains on the sliding surface and satisfies the previous conditions.

The main objective of this study is to formulate control laws that drive the error between the system's current state and the desired trajectory (delayed state) to zero. Based on the Lyapunov theorem, the necessary and sufficient condition for the system (3.1) to satisfy the reachability condition is expressed as follows:

$$\begin{aligned} &\frac{1}{2}\frac{d}{dt}\left(S^2\right) \leqslant 0 \\ &\Longrightarrow S^T\dot{S} \leqslant 0 \end{aligned} \tag{3.5}$$

with $S = \begin{bmatrix} S_1 & S_2 & \cdots & S_n \end{bmatrix}^T$.

It is ensured by condition (3.5) that the system state trajectory always reaches the sliding surface. The following is a stricter reachability requirement known as the "δ-condition" [20]:

$$\begin{aligned} &S^T\dot{S} \leqslant -\delta|S| \\ &\Longrightarrow \dot{S} \leqslant -\delta_i \operatorname{sgn}(S_i), \end{aligned} \tag{3.6}$$

where sgn is the signum function and δ_i $(i = 1, 2, \ldots, n)$ are strictly positive constants.

We calculate the time derivative of S and substitute it into Eq. (3.6) to get

$$\ddot{e}_i + \lambda_i \dot{e}_i \leqslant -\delta_i \operatorname{sgn}(S_i). \tag{3.7}$$

In order to ensure the stability of the closed-loop system and to handle the uncertainties and disturbances of the system, the sliding mode control laws u_{si} $(i = 1, 2, \ldots, n)$ are created to guide the dynamics of the system towards sliding surfaces $(S(t) = 0)$. Thus, the sliding mode control laws are:

$$u_{si} = -S_i - \delta_i \operatorname{sign}(S_i). \tag{3.8}$$

3.1. Control with one sliding surface

In this section, the main problem to be addressed is how to utilize a single sliding mode surface to achieve synchronization between the present state and the delayed one of the Rössler system with a delay of one period of time.

To achieve the desired synchronization, the master and slave Rössler systems are described by the differential Eqs. (3.9) and (3.10), respectively.

The master system is

$$\begin{cases} \dot{x}(t-\tau) = -y(t-\tau) - z(t-\tau), \\ \dot{y}(t-\tau) = x(t-\tau) + ay(t-\tau), \\ \dot{z}(t-\tau) = b + z(t-\tau)(x(t-\tau) - c), \end{cases} \tag{3.9}$$

and the slave system is

$$\begin{cases} \dot{x}(t) = -y(t) - z(t), \\ \dot{y}(t) = x(t) + ay(t), \\ \dot{z}(t) = b + z(t)(x(t) - c) + u(t), \end{cases} \tag{3.10}$$

where $(x(t-\tau),\, y(t-\tau),\, z(t-\tau))$, $(x(t),\, y(t),\, z(t))$ are the states of the systems (3.9) and (3.10), respectively, τ is the time delay equal to the period of the target UPO, and $u(t)$ is the control action.

The synchronization error between the master (3.9) and the slave (3.10) can be expressed as

$$\begin{cases} e_1(t) = x(t) - x(t-\tau), \\ e_2(t) = y(t) - y(t-\tau), \\ e_3(t) = z(t) - z(t-\tau). \end{cases} \tag{3.11}$$

Its time derivative is

$$\begin{cases} \dot{e}_1(t) = \dot{x}(t) - \dot{x}(t-\tau), \\ \dot{e}_2(t) = \dot{y}(t) - \dot{y}(t-\tau), \\ \dot{e}_3(t) = \dot{z}(t) - \dot{z}(t-\tau) \end{cases} \tag{3.12}$$

$$\Longrightarrow \begin{cases} \dot{e}_1(t) = -e_2(t) - e_3(t), \\ \dot{e}_2(t) = e_1(t) + ae_2(t), \\ \dot{e}_3(t) = e_1(t)e_3(t) + z(t-\tau)e_1(t) + x(t-\tau)e_3(t) - ce_3(t) + u(t). \end{cases} \tag{3.13}$$

Now, the controller $u(t)$ can be defined as follows:

$$u(t) = u_{eq}(t) + u_{sw}(t). \tag{3.14}$$

According to [20], we can redefine the sliding surface as

$$s = \sum_{i=0}^{n} \lambda_i e_i(t). \tag{3.15}$$

Then:

$$s = \lambda_1 e_1(t) + \lambda_2 e_2(t) + \lambda_3 e_3(t), \tag{3.16}$$

where λ_1, λ_2, and λ_3 are constant parameters.

The equivalent control $u_{eq}(t)$ is determined by the condition that the derivative of the sliding surface ($\dot{s}$) is zero. This control action helps to drive the system towards the sliding surface. The control input (u_{sw}) is designed for the error dynamics in a way that satisfies the reaching condition $s(t)\dot{s}(t) < 0$, which ensures the sliding motion on the sliding surface ($s(t) = 0$).

When the system operates in sliding mode, it satisfies the following conditions [15, 18]:

$$\begin{cases} s(t) = 0, \\ \dot{s}(t) = 0. \end{cases} \tag{3.17}$$

By deriving Eq. (3.16) with respect to time and replacing the $\dot{e}_1$, $\dot{e}_2$ and $\dot{e}_3$ values from Eq. (3.13), we get

$$\begin{aligned} \dot{s}(t) = \lambda_1 \dot{e}_1(t) + \lambda_2 \dot{e}_2(t) + \lambda_3 \dot{e}_3(t) = \lambda_1(-e_2(t) - e_3(t)) + \lambda_2(e_1(t) + ae_2(t)) + \\ + \lambda_3(e_1(t)e_3(t) + z(t-\tau)e_1(t) + x(t-\tau)e_3(t) - ce_3(t) + u_{eq}(t)). \end{aligned} \tag{3.18}$$

Consequently, when the system operates in the sliding manifold and the derivative of the sliding surface ($\dot{s}(t)$) is equal to zero, the equivalent control (u_{eq}), in the sliding mode, is given by

$$\begin{aligned} u_{eq}(t) = \frac{1}{\lambda_3}[-\lambda_1(-e_2(t) - e_3(t)) - \lambda_2(e_1(t) + \\ + ae_2(t)) - \lambda_3(e_1(t)e_3(t) + z(t-\tau)e_1(t) + x(t-\tau)e_3(t) - ce_3(t)]. \end{aligned} \tag{3.19}$$

Next, the control action (u_{sw}) is designed as follows:

$$u_{sw}(t) = -\delta \cdot \mathrm{sign}(s), \tag{3.20}$$

where δ is a positive constant and $\mathrm{sign}(\cdot)$ is the signum function.

Theorem 1. *Using the control actions* (u_{eq}) *and* (u_{sw}) *detailed in Eqs.* (3.19) *and* (3.20)*, respectively, in addition to the proposed surface given by Eq.* (3.16)*, the controller* $u(t)$ *that ensures the closed-loop system asymptotic stability can be expressed as follows*:

$$\begin{aligned} u(t) = u_{eq}(t) + u_{sw}(t) = \frac{1}{\lambda_3}[-\lambda_1(-e_2(t) - e_3(t)) - \lambda_2(e_1(t) + ae_2(t)) - \\ - \lambda_3(e_1(t)e_3(t) + z(t-\tau)e_1(t) + x(t-\tau)e_3(t) - ce_3(t)] - \delta \cdot \mathrm{sign}(s). \end{aligned} \tag{3.21}$$

Proof. By selecting an appropriate Lyapunov function, we can analyze the stability properties of the proposed control and ensure that the system's trajectories converge towards the desired sliding surface. To this end, we introduce the Lyapunov function defined as follows:

$$V = \frac{1}{2}s^2. \tag{3.22}$$

By evaluating its time derivative along the trajectory described by (3.16), we obtain

$$\begin{aligned}\dot{V} = s\dot{s} = s[\lambda_1\dot{e}_1(t) + \lambda_2\dot{e}_2(t) + \lambda_3\dot{e}_3(t)] = s[\lambda_1(-e_2(t) - e_3(t)) + \lambda_2(e_1(t) + ae_2(t)) + \\ + \lambda_3(e_1(t)e_3(t) + z(t-\tau)e_1(t) + x(t-\tau)e_3(t) - ce_3(t) + u(t))] = \\ = s\left\{\lambda_1[-e_2(t) - e_3(t)] + \lambda_2[e_1(t) + ae_2(t)] + \right. \\ + \lambda_3\left[e_1(t)e_3(t) + z(t-\tau)e_1(t) + x(t-\tau)e_3(t) - ce_3(t) + \right. \\ + \left.\left(\frac{1}{\lambda_3}[-\lambda_1(-e_2(t) - e_3(t)) - \lambda_2(e_1(t) + ae_2(t))(t)e_3(t) - \right.\right. \\ \left.\left.\left. -\lambda_3(e_1(t)e_3(t) + z(t-\tau)e_1(t) + x(t-\tau)e_3(t) - ce_3(t))] - \delta\cdot\operatorname{sign}(s)\right)\right]\right\} = \\ = s[-\delta\cdot\operatorname{sign}(s)] = -\delta\cdot|s|.\end{aligned} \tag{3.23}$$

As $\delta > 0$, we have $\dot{V} < 0$, and based on Lyapunov stability theory [16], it can be concluded that the error dynamics system (3.11) under the controller $u(t)$ given by (3.21) is asymptotically stable. □

3.2. Control with three sliding surfaces

In this section, we address the problem of synchronizing the Rössler system's present state with its delayed state by one period using three-sliding surfaces. The Rössler system (2.1) can be written as follows:

$$\begin{cases}\dot{x}(t) = -y(t) - z(t) + u_1(t), \\ \dot{y}(t) = x(t) + ay(t) + u_2(t), \\ \dot{z}(t) = b + z(t)(x(t) - c) + u_3(t).\end{cases} \tag{3.24}$$

The derivative of the synchronization errors vector between the present state and the delayed one can be expressed as

$$\begin{cases}\dot{e}_1(t) = -e_2(t) - e_3(t) + u_1(t), \\ \dot{e}_2(t) = e_1(t) + ae_2(t) + u_2(t), \\ \dot{e}_3(t) = e_1(t)e_3(t) + z(t-\tau)e_1(t) + x(t-\tau)e_3(t) - ce_3(t) + u_3(t).\end{cases} \tag{3.25}$$

We insert e_i and $\dot{e}_i$ into Eq. (3.4) to define the sliding surfaces as follows:

$$\begin{cases}s_1(t) = \dot{e_1}(t) + \lambda_1 e_1(t), \\ s_2(t) = \dot{e_2}(t) + \lambda_2 e_2(t), \\ s_3(t) = \dot{e_3}(t) + \lambda_3 e_3(t),\end{cases} \tag{3.26}$$

where λ_1, λ_2 and λ_3 are positive real numbers.

Theorem 2. *Based on the principles established by Eq.* (3.7) *and taking into consideration the sliding surfaces characterized in Eq.* (3.26)*, the closed-loop system asymptotic stability can be effectively ensured by the following control law*:

$$\begin{cases} u_1(t) = -\lambda_1 e_1 + e_2 + e_3 - \delta\,\mathrm{sign}(s_1), \\ u_2(t) = -\lambda_2 e_2 - e_1 - a e_2 - \delta\,\mathrm{sign}(s_2), \\ u_3(t) = -\lambda_3 e_3 - e_1 e_3 - z(t-\tau)e_1 - x(t-\tau)e_3 + c e_3 - \delta\,\mathrm{sign}(s_3). \end{cases} \tag{3.27}$$

Proof. The Lyapunov function serves as a crucial tool for substantiating the stability and showing the eventual convergence of the synchronization errors to zero. Thus, we introduce the Lyapunov function:

$$V(t) = \frac{1}{2}\left(e_1(t)^2 + e_2(t)^2 + e_3(t)^2\right). \tag{3.28}$$

The time derivative of the above equation is

$$\dot{V}(t) = \dot{e}_1 e_1 + \dot{e}_2 e_2 + \dot{e}_3 e_3. \tag{3.29}$$

By substituting the proposed control (3.27) into Eq. (3.25) and $\dot{e}_1$, $\dot{e}_2$ and $\dot{e}_3$ into Eq. (3.29), the resulting expression is

$$\dot{V}(t) = -\lambda_1 e_1^2 - \lambda_2 e_2^2 - \lambda_3 e_3^2 - \delta[|s_1| + |s_2| + |s_3|]. \tag{3.30}$$

With the positive integer values assigned to λ_1, λ_2, λ_3 and δ, the Lyapunov function condition, as indicated by $\dot{V} < 0$, is satisfied [16]. This adherence to the principles of Lyapunov stability theory allows us to confidently assert both the system's asymptotic stability and the convergence of the synchronization errors to zero. □

3.3. Control with three integral sliding surfaces

As described in the previous section (Section 3.2), the control law is constructed using three surfaces, and for the definition of a sliding surface, we utilize suitable proportional-integral (PI) sliding surfaces.

The PI sliding surface is a type of sliding surface that incorporates both proportional and integral components. It is designed in the framework of regulating the synchronization error between the current state and the desired delayed state of the Rössler system. The proportional component helps to respond to the instantaneous error between the two states, while the integral component deals with the accumulated error over time. Hence, the proportional-integral (PI) sliding surface is

$$s_i(t) = e_i(t) + \lambda_i \int_0^t e_i(\alpha)\, d\alpha, \tag{3.31}$$

where λ_i are positive real numbers and α is the integral variable. In the same context, we can express the switching surfaces in the following manner:

$$\begin{cases} s_1(t) = e_1(t) + \lambda_1 \int\limits_0^t e_1(\alpha)\, d\alpha, \\ s_2(t) = e_2(t) + \lambda_2 \int\limits_0^t e_2(\alpha)\, d\alpha, \\ s_3(t) = e_3(t) + \lambda_3 \int\limits_0^t e_3(\alpha)\, d\alpha. \end{cases} \tag{3.32}$$

The time derivatives of the sliding surfaces are given by

$$\begin{cases} \dot{s}_1(t) = \dot{e}_1(t) + \lambda_1 e_1(t), \\ \dot{s}_2(t) = \dot{e}_2(t) + \lambda_2 e_2(t), \\ \dot{s}_3(t) = \dot{e}_3(t) + \lambda_3 e_3(t). \end{cases} \tag{3.33}$$

While the system operates in sliding mode, it conforms to the specified conditions ($\dot{s}_i(t) = 0$). This signifies:

$$\Longrightarrow \begin{cases} \dot{e}_1(t) = -\lambda_1 e_1(t), \\ \dot{e}_2(t) = -\lambda_2 e_2(t), \\ \dot{e}_3(t) = -\lambda_3 e_3(t). \end{cases} \tag{3.34}$$

We notice that the first derivative of the error $\dot{e}_i(t)$ divided by the error $e_i(t)$ is less than zero because $\lambda_i > 0$, which means that the function of the error is decreasing.

Theorem 3. *By implementing the controller defined in Eq.* (3.35) *and incorporating the proposed proportional integral sliding surfaces from Eq.* (3.32)*, the asymptotic stability of the closed-loop system is guaranteed. Furthermore, the synchronization errors converge asymptotically to zero*:

$$\begin{cases} u_1(t) = -\lambda_1 e_1 + e_2 + e_3 - \delta\, \mathrm{sign}(s_1), \\ u_2(t) = -\lambda_2 e_2 - e_1 - a e_2 - \delta\, \mathrm{sign}(s_2), \\ u_3(t) = -\lambda_3 e_3 - e_1 e_3 - z(t-\tau) e_1 - x(t-\tau) e_3 + c e_3 - \delta\, \mathrm{sign}(s_3), \end{cases} \tag{3.35}$$

where λ_1, λ_2, λ_3 and δ must be positive and correctly selected and $\mathrm{sign}(\cdot)$ *is the signum function.*

Proof. To confirm the convergence of the synchronization errors to zero, we conducted an analysis of the Lyapunov stability conditions.

We choose the Lyapunov function as follows:

$$V(t) = \frac{1}{2}\left(e_1(t)^2 + e_2(t)^2 + e_3(t)^2\right). \tag{3.36}$$

Using the time derivative of the above equation, we obtain

$$\dot{V}(t) = \dot{e}_1 e_1 + \dot{e}_2 e_2 + \dot{e}_3 e_3. \tag{3.37}$$

Substituting $\dot{e}_1$, $\dot{e}_2$ and $\dot{e}_3$ from Eq. (3.34) into Eq. (3.37), we get

$$\dot{V(t)} = -\lambda_1 e_1^2 - \lambda_2 e_2^2 - \lambda_3 e_3^2. \tag{3.38}$$

According to the Lyapunov stability theory [16], the values of λ_1, λ_2, and λ_3 in (3.38) must be chosen in such a manner that $\dot{V}(t) < 0$ in order to guarantee the asymptotic stability of the sliding manifold. As a result, we may state that λ_1, λ_2, and λ_3 must all have positive integer values for the asymptotic stability requirement. □

4. Simulation results

We maintain the Rössler system (2.1) with the initial conditions chosen arbitrarily as [0.2, 0.2, 0.2], and the parameter values $[a, b, c] = [0.2, 0.2, 5.7]$. The value of the time delay τ that matches the first period of UPO is $\tau = T_1 = 5.88105$.

4.1. Simulation with the first controller

The controller $u(t)$ (3.21) is activated at time $t = 150$ s with parameter values λ_1, λ_2, λ_3, and δ equal to 2, 2, 0.04 and 0.2, respectively.

The resulting time evolution of the system is depicted in Fig. 3, the time response $x(t)$, $y(t)$ and $z(t)$ is shown in Fig. 4 and the controller action $u(t)$ is represented in Fig. 5.

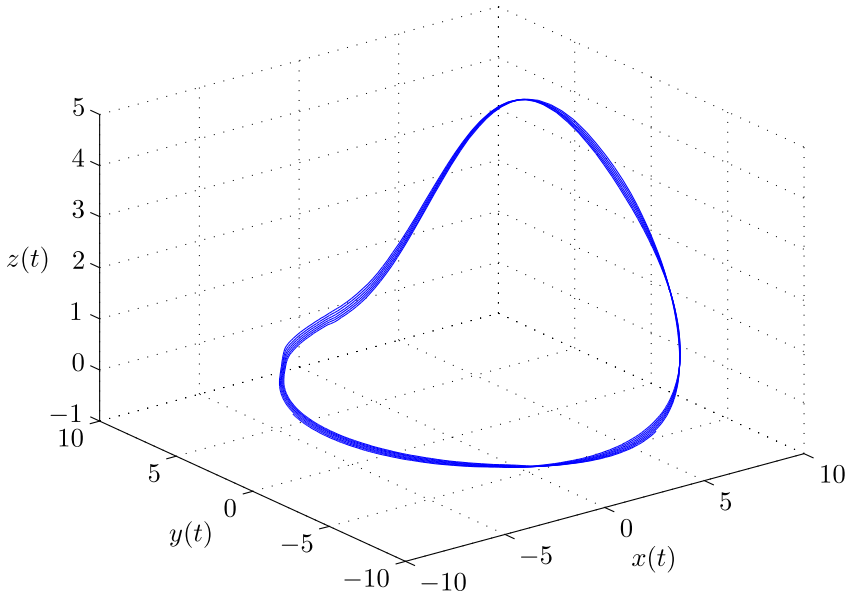

Fig. 3. Behavior of the Rössler system under the 1^{st} controller

Figure 3 shows that the behavior of the system follows a single and periodic pattern, which is the simplest and the most predictable behavior exhibited by a dynamical system. To provide a more comprehensive understanding, Fig. 4 illustrates the time behavior of the system. This figure presents a visual representation of how the system evolves and behaves over time.

Once the stabilization process is guaranteed, as depicted in Fig. 5, it can be observed that the control signal converges to zero, indicating a successful structural stabilization of the Rössler system.

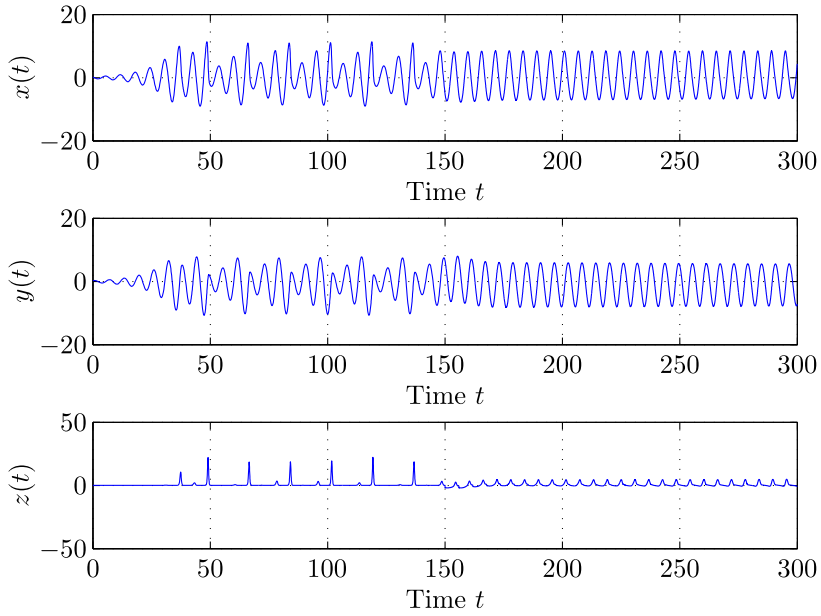

Fig. 4. Time response $x(t)$, $y(t)$ and $z(t)$ under the 1^{st} controller

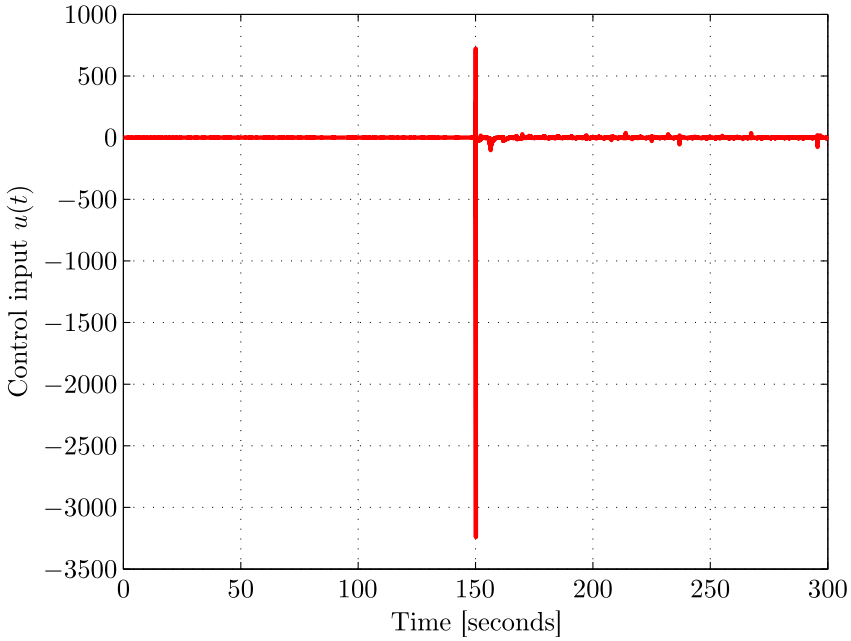

Fig. 5. 1^{st} controller action

4.2. Simulation with the second controller

We activate the proposed controller (3.27) at $t = 150$ s with the values of λ_1, λ_2, λ_3 and δ equal to 60, 40, 400 and 0.05, respectively.

The resulting time evolution of the system is depicted in Fig. 6 and the time evolution of $x(t)$, $y(t)$ and $z(t)$ is illustrated in Fig. 7, while the controller signals u_1, u_2 and u_3 are given in Fig. 8.

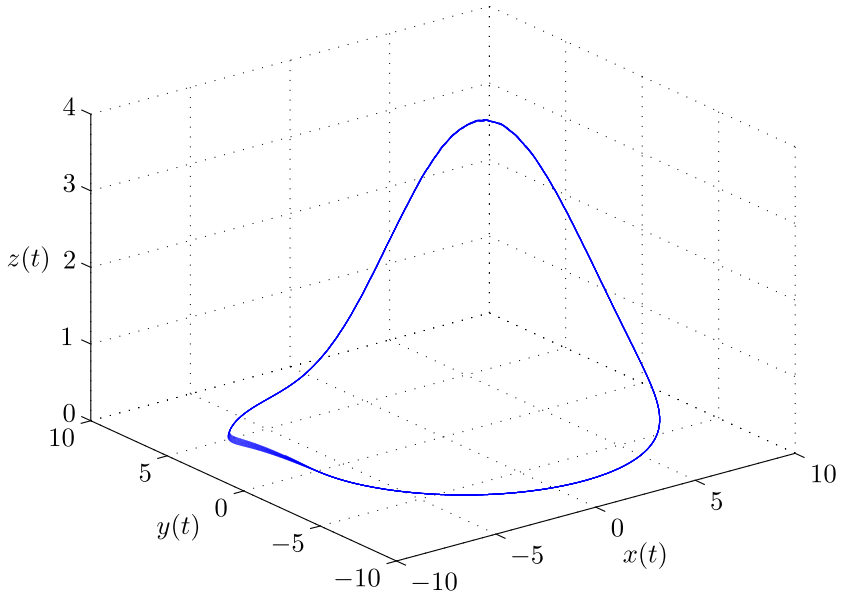

Fig. 6. Behavior of the Rössler system under the 2^{nd} controller with $\tau = T_1 = 5.88$

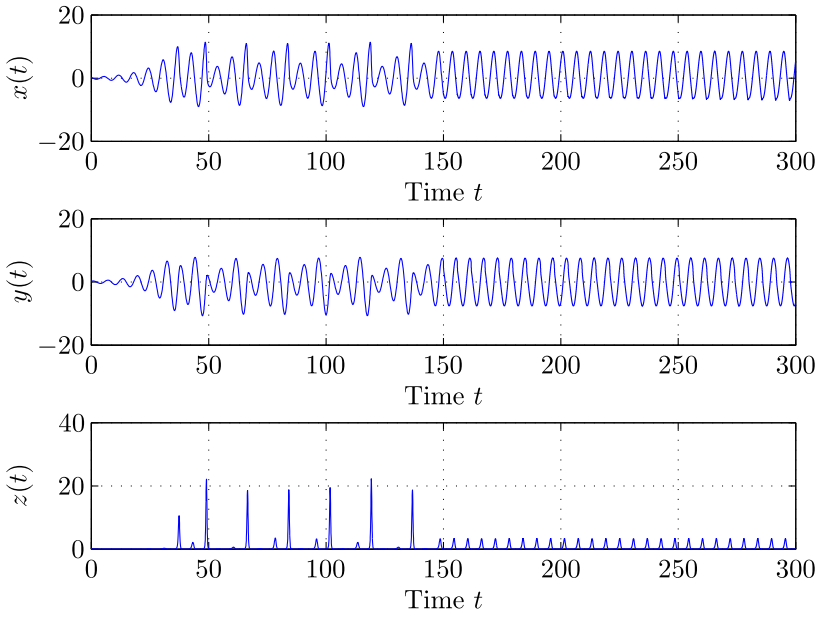

Fig. 7. Evolution of the states $x(t)$, $y(t)$ and $z(t)$ under the 2^{nd} controller

The results presented in Fig. 6 indicate that the system behavior is periodic and exhibits a single-period response. To provide a clearer illustration of the system's behavior, Fig. 7 depicts the time behavior of the system before and after activating the proposed controller (3.27). When the controller is activated at $t = 150$ s, the system is rapidly stabilized during the first period, and the Rössler system's general behavior becomes periodic. As can be seen from Fig. 8, when the stabilization process is completed, the control signal becomes zero.

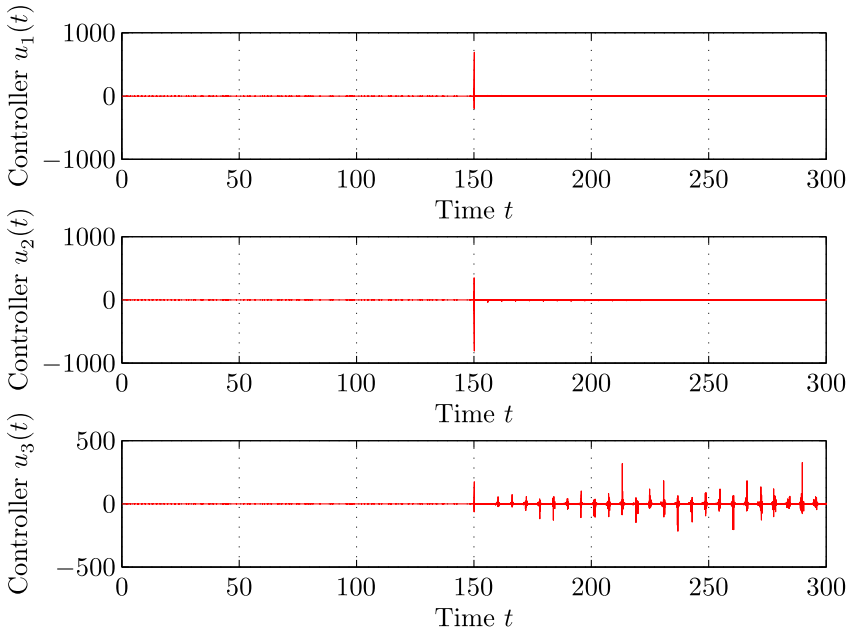

Fig. 8. Control actions u_1, u_2 and u_3 of the 2^{nd} controller

4.3. Simulation with the third controller

Similarly to the previous simulation, we activate the proposed controller (3.38) at $t = 150$ s with the values of parameters λ_1, λ_2, λ_3 and δ satisfying the stability condition (3.37) and equal to 50, 10, 10 and 0.05, respectively.

The resulting time evolution of the system, time response $x(t)$, $y(t)$ and $z(t)$ and the controller signals u_1, u_2 and u_3 are represented in Figs. 9, 10, and 11, respectively.

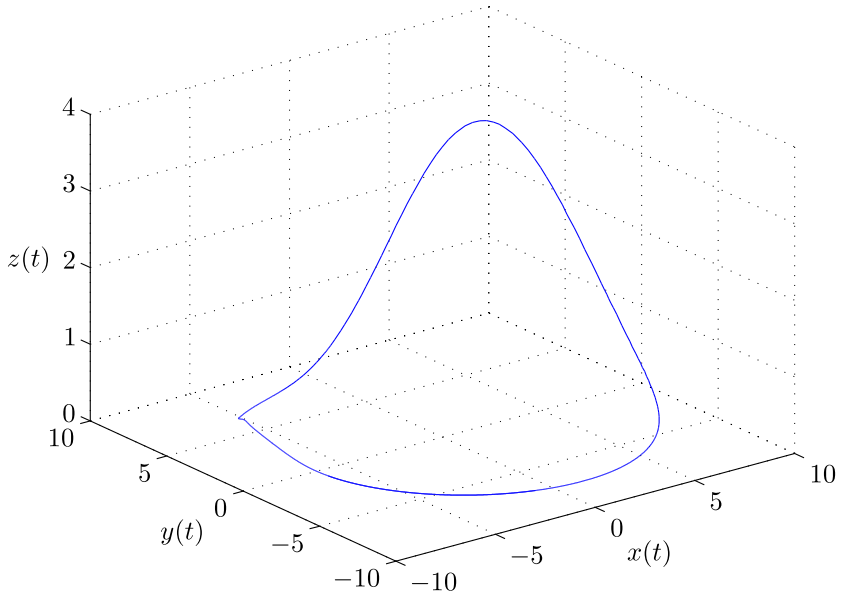

Fig. 9. Behavior of the Rössler system under the 3^{rd} controller

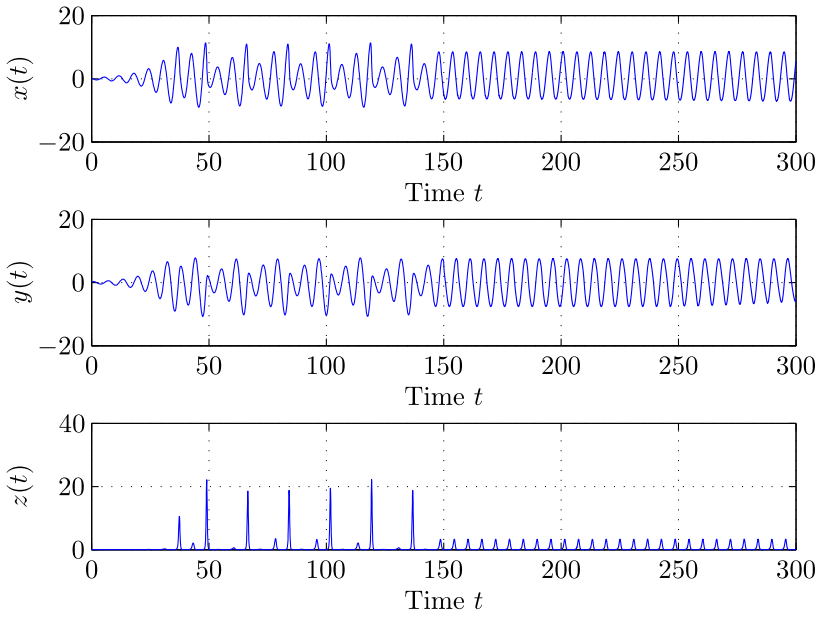

Fig. 10. Evolution of the states $x(t)$, $y(t)$ and $z(t)$ under the 3^{rd} controller

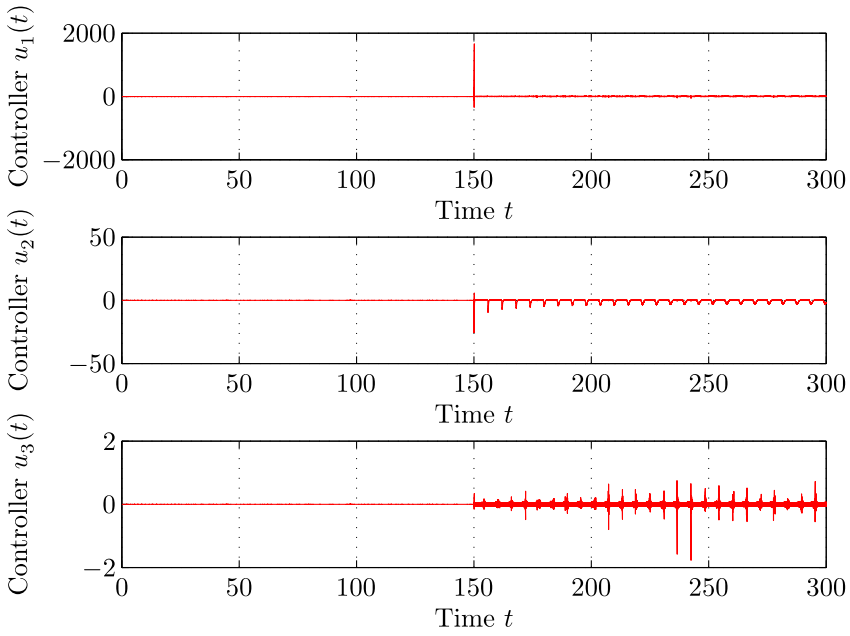

Fig. 11. Control actions u_1, u_2 and u_3 under the 3^{rd} controller

It is remarkable that the results presented in Figs. 9, 10, and 11 are consistent and identical, respectively, to Figs. 6, 7 and 8 shown in the previous part. This indicates that the delayed sliding-mode control approach consistently demonstrates its effectiveness in stabilizing the considered benchmark system and achieving synchronization, even with changes in the sliding surface.

For a straightforward comparison between the three simulations, it is obvious that the performance of control utilizing the three control laws surpasses that of employing a single

controller. On a different note, when evaluating the execution times of the three proposed approaches, we find values of $t_1 = 3.5$ s, $t_2 = 1260$ s, and $t_3 = 173$ s, respectively. This indicates that the execution time for the three sliding surfaces is longer than that of the three integral sliding surfaces and the single sliding surface. Consequently, based on these observations, we conclude that employing three integral sliding surfaces not only enhances control performance, but also accelerates the computation speed.

Overall and based on the outcomes of the three simulations conducted in this study, it is evident that the proposed delayed sliding-mode control methods exhibit a high level of effectiveness in mastering the behavior of the chaotic system towards a simple periodic behavior. The efficiency of the control approach remains consistent regardless of the chosen control activation point, as it remains flexible enough to be engaged at any time. This adaptability underscores the robustness and versatility of the approach in achieving its intended outcomes, regardless of the control activation instant. The proposed approaches are characterized by their rapid and effective stabilization aspect over a period of time during any unstable periodic orbit (UPOs). These results provide strong support for the effectiveness of the proposed delayed sliding-mode control approaches in stabilizing chaotic systems and achieving synchronization between the current state and the desired delayed one. The ability to achieve rapid stabilization and subsequent periodic behavior shows the profound ability of the proposed control approaches to effectively regulate and control the unpredictable and erratic behaviors of complex chaotic systems.

5. Conclusion

This paper presents a comprehensive investigation of delayed sliding-mode-based approaches for chaos control or elimination in complex and chaotic systems. The closed-loop stability of the system is proven based on Lyapunov theory, and the bridge between classical stability and structural stability is built through the transformation of the tracking error into a synchronization error.

Through the simulation results, we have validated and shown the effectiveness of the proposed control approaches in driving the chaotic system toward stable and simple periodic behavior. The results have confirmed that the proposed delayed sliding-mode control method is capable of rapidly achieving stabilization, even with changes in the sliding surface and/or the activation time point. This fact endorsed the adaptability and reliability of the proposed approaches. The controlled system exhibited remarkable insensitivity to changes in initial conditions, which shows the robustness of the proposed approaches. They consistently stabilized the chaotic system and ensured the simplest and most predictable behavior of the system.

Conflict of interest

The authors declare that they have no conflict of interest.

References

[1] Strogatz, S., *Nonlinear Dynamics and Chaos: With Applications to Physics, Biology, Chemistry, and Engineering,* 2nd ed., Boca Raton, Fla.: CRC, 2015.

[2] Pyragas, K., Continious Control of Chaos by Self-Controlling Feedback, *Phys. Lett. A,* 1992, vol. 170, no. 6, pp. 421–428.

[3] Zhang, L. and Yan, Y., Discrete Active Model Predictive Control of Continuous Unified Chaotic System, in *Proc. of the Chinese Control and Decision Conf. (CCDC, Nanchang, China, 2019),* pp. 3390–3394.

[4] Medhaffar, H., Feki, M., and Derbel, N., Adaptive Fuzzy Control for the Stabilisation of Chaotic Systems, *Int. J. Autom. Control,* 2020, vol. 14, no. 2, pp. 115–137.

[5] Hamidouche, B., Guesmi, K., and Essounbouli, N., Lyapunov Exponent-Based PI Optimization for the Delayed Feedback Control of Chaos, in *Proc. of the Internat. Conf. of Advanced Technology in Electronic and Electrical Engineering (ICATEEE, M'sila, Algeria, 2022),* 5 pp.

[6] Li, X. and Zhu, C., Saturated Impulsive Control of Nonlinear Systems with Applications, *Automatica J. IFAC,* 2022, vol. 142, Paper No. 110375, 5 pp.

[7] Hosseinabadi, P. A. and Abadi, A. S. S., Adaptive Terminal Sliding Mode Control of High-Order Nonlinear Systems, *Int. J. Autom. Control,* 2019, vol. 13, no. 6, pp. 668–678.

[8] Cao, Q. and Wei, D. Q., Dynamic Surface Sliding Mode Control of Chaos in the Fourth-Order Power System, *Chaos Solitons Fractals,* 2023, vol. 170, Paper No. 113420, 6 pp.

[9] Tiwari, A. and Handa, H., Sliding Mode Control for Rossler Prototype-4 System Using Two and Three Controllers, in *Proc. of the 7th Internat. Conf. on Signal Processing and Integrated Networks (SPIN, Noida, India, 2020),* pp. 1095–1099.

[10] *Applications of Sliding Mode Control in Science and Engineering,* S. Vaidyanathan, Ch.-H. Lien (Eds.), Stud. in Comput. Intel., vol. 709, Cham: Springer, 2017.

[11] Liu, D. and Yamaura, H., Stabilization Control for Giant Swing Motions of 3-Link Horizontal Bar Gymnastic Robot Using Multiple-Prediction Delayed Feedback Control with a Periodic Gain, *J. Syst. Des. Dyn.,* 2011, vol. 5, no. 1, pp. 42–54.

[12] Rössler, O. E., An Equation for Continuous Chaos, *Phys. Lett. A,* 1976, vol. 57, no. 5, pp. 397–398.

[13] Wolf, A., Swift, J. B., Swinney, H. L., and Vastano, J. A., Determining Lyapunov Exponents from a Time Series, *Phys. D,* 1985, vol. 16. no. 3, pp. 285–317.

[14] Li, J., Cao, J., and Liu, H., State Observer-Based Fuzzy Echo State Network Sliding Mode Control for Uncertain Strict-Feedback Chaotic Systems without Backstepping, *Chaos Solitons Fractals,* 2022, vol. 162, Paper No. 112442, 11 pp.

[15] *Applications of Sliding Mode Control in Science and Engineering,* S. Vaidyanathan, Ch.-H. Lien (Eds.), Stud. in Comput. Intel., vol. 709, Cham: Springer, 2017.

[16] Khalil, H. K., *Nonlinear Systems,* 3rd ed., Upper Saddle River, N.J.: Prentice Hall, 2002.

[17] Slotine, J.-J. E. and Li, W., *Applied Nonlinear Control,* Englewood Cliffs, N.J.: Prentice Hall, 1991.

[18] Utkin, V. I., *Sliding Modes and Their Application in Variable Structure Systems,* Moscow: Mir, 1978.

[19] *Applications of Sliding Mode Control,* N. Derbel, J. Ghommam, Q. Zhu (Eds.), Stud. Syst. Decis. Control, vol. 79, Singapore: Springer, 2017.

[20] Liu, J., Gao, Y., Yin, Y., Wang, J., Luo, W., and Sun, G., *Sliding Mode Control Methodology in the Applications of Industrial Power Systems,* Studies in Systems, Decision and Control, vol. 249, Cham: Springer, 2020.